Frequency 3D Mapping and Inter-Channel Stability of EEG Intrinsic Function Pulsation : Indicators Towards Autism Spectrum Diagnosis

Enas Abdulhay*†[a], Maha Alafeef †[a], Hikmat Hadoush[b]
[a] Biomedical Engineering department
[b]Rehabilitation Sciences department
Jordan University of Science and Technology
Irbid, Jordan

Natheer Alomari, Mo'ath Bashayreh
Neurology Department
King Abdullah University Hospital
Irbid, Jordan

Abstract- Autism spectrum is one of the serious disorders influencing mental capacities and hence behavior. The present work investigates the potential of detecting irregularities of EEG activity and connectivity in Autism Spectrum by studying the inter-channel stability of EEG components point-by-point pulsation as well as by frequency 3D mapping. First, Empirical Mode Decomposition is used to find the Intrinsic Mode Functions of every EEG channel. Second, the Phase derivatives of analytic intrinsic modes are then calculated. Third, each phase derivative function obtained for an intrinsic mode is plotted versus the phase derivative function of the counterpart intrinsic mode in another channel. Finally, the stability loops found out are then analyzed. Furthermore, 3D mapping of EEG frequency bands (Delta, Theta, Alpha and Beta) is conducted and examined.

Keywords—Autism; EEG;, channel; IMF; phase; stability; frequency; mapping.

I. INTRODUCTION

With onset in the first years of life, autism presents as a disorder of profound social disconnect rooted in early brain development. According to the American DSM-IV manual, the autism behavioral diagnosis involves deficits in three areas: (1) shared social interactions, (2) language and communication, (3) restricted or repetitive patterns of behavior and interests. Deficits in Autism mainly occur in processes that demand integration of information as well as coordination of multiple neural systems such as language and social interaction [1].

Many techniques can be used to visualize brain activity including functional magnetic resonance imaging (fMRI), positron emission tomography (PET); single-photon emission computed tomography (SPECT), magnetic resonance spectroscopy (MRS), hemoencephalography (HEG), magnetoencephalography (MEG), transcranial magnetic stimulation (TMS), event related optical signals (EROS) as well as continuous and event-related electroencephalography (EEG). However, diagnosing a child with autism has been a difficult process. Many factors including acquisition parameters, details of image processing, feature extraction procedures and analytic methods contribute significantly in conflicting findings of imaging techniques attempted for Autism Spectrum diagnosis. The disparities are also induced by the imaging protocols and the difficulty of linking the abnormalities to the clinical symptomatology. There are therefore no medical tests capable of detecting the disorder; and current screening methods tend to rely solely on analyzing a child's behavior [2].

Historically, clinical EEG applications were limited to the detection of epileptic seizures [8], localization of the seizure foci, brain injury, and the study of sleep disorders. However, recently, several studies have demonstrated that the mathematical processing of digitally recorded EEG can provide important information about functional interactions between neural systems [6-7,10]. EEG has many advantages: It is portable, measures the brain electrical activity directly, can be used for hours, inexpensive, user-friendly, non-disturbing, convenient for a wide range of age groups, less noisy, tolerant to movement, has high temporal resolution, has a good spatial resolution when it is used for brain mapping, clinically available, non-invasive and can be used to collect repeated measurements.

The recent studies depend on linear methods like Fourier transform [4] or wavelets [11] in application to Autism nonlinear non-stationary details. This decreases obtained accuracy [12].

The present work focuses on the mathematical calculation of EEG key features: (1) Inter-channel stability of counterpart Intrinsic Mode Functions pulsation as well as (2) frequency 3D mapping. Alterations of the aforementioned EEG features between autistic children and neuro-typical controls are studied. First, the nonlinear Empirical Mode Decomposition method is used to find the Intrinsic Mode Functions (IMFs) of every EEG channel. Second, the point-by-point phase derivatives (pulsation) of analytic intrinsic modes are then calculated. Third, each phase derivative function obtained for an intrinsic mode is plotted versus the phase derivative function

[1] *: corresponding author : ewabdulhay@just.edu.jo
[2] †: equal contribution
[3] This study is funded by the Scientific Research Support Fund, Jordan

of the counterpart intrinsic mode in another channel. Finally, the stability loops found out are analyzed to search for abnormal neural connectivity between brain zones. In addition, 3D mapping of EEG frequency bands (Delta, Theta, Alpha and Beta) is conducted and examined to search for abnormal EEG activities. The used key features will be shown to serve as preliminary indicators of Autism.

II. Materials and Methods

A. Volunteers

The EEG signals of ten autistic (5 females and 5 males) and ten neuro-typical children (5 females and 5 males) were studied. The age varied from 4 to 13. The autistic children were recruited from national centers and had been diagnosed by experts according to international standards. All selected autistic children do not suffer from any other concurrent neurological disorders and do not take medications.

Every parent has signed a consent form for his child. The recording has been approved ethically by the IRB committee of Jordan University of Science and Technology/King Abdullah University Hospital.

B. EEG Recording

Every child has been asked to sit properly and quietly, by concentrating on a fixed screen, for 25 minutes. Afterwards, the EEG technician placed the 64 channel cap (Waveguard, ANT Neuro) with the suitable size and according to the international 10-20 system, connected it to the amplifier (ES-232, ANT Neuro), checked up the values of the impedance for every electrode via the licensed recording software (eego sports 64), visualized the EEG signals of the different channels, and finally started the resting state recording with a 500Hz sampling frequency. During the recording, the technician added events marks (e.g. eye blinking, crying .etc) when necessary.

C. EEG Processing

Filtering and pre-processing: The acquired EEG signals were band-pass filtered to achieve the range 0.3-40 Hz. All artifacts and eye movements were inspected and eliminated by the Independent Component Analysis method via the software LA-106 ASA ERP as well as by a neurologist.

EEG decomposition: For every child, every EEG channel was processed by the Empirical Mode Decomposition method (EMD) to extract the Intrinsic Mode Functions. EMD [9] is a nonlinear adaptive method able of decomposing a nonlinear non-stationary signal to its main oscillatory components.

In Intrinsic Mode Function, the extrema and zero crossings numbers differ by one at maximum. In addition, there should be no difference between the local average of the upper and lower envelopes. The procedure of EMD is: (1) Detection of the maxima and minima. (2) Calculation of interpolated upper and lower envelopes as well as of local instantaneous mean of envelopes. (3) Subtraction of the obtained local mean from the signal. The outcome of step 3 named the ‘’detail’’ should satisfy the aforementioned two conditions in order to be considered as an Intrinsic Function. Otherwise, the steps 1-3 should be re-conducted. In our work, the maximum allowed number of iterations (repetitions) is 2000. (4) Applying steps 1-3 to ((original signal) + (– detail)) for the computation of the following IMFs. (5) The IMFs are considered as the achieved details and the final residual.

In the present paper, EMD of obtained EEG signals has been realized by MATLAB.

D. Feature calculation

Analytic IMF: The analytic IMF can be calculated by the following formula:

$$Anal = \mathrm{Re}al + [\frac{1}{\pi}\lim_{\in \to 0^+}(\int_{t-1/\in}^{t-\in} \frac{\mathrm{Re}al(\tau)}{t-\tau}d\tau + \int_{t+\in}^{t+1/\in} \frac{\mathrm{Re}al(\tau)}{t-\tau}d\tau)]\, i \tag{1}$$

where the real part is the IMF.

Local point-by-point pulsation: Local point-by-point pulsation values for every analytic IMF is then found out [8, 9]. The point-by-point pulsation is calculated as the derivative of the point-by-point phase of the analytic IMF. The point-by-point phase of the analytic IMF is calculated as the inverse TAN function of (Imaginary/Real).

Stability loop: The point-by-point pulsation function values for every IMF of every channel is plotted versus the point-by-point pulsation function values of the counterpart IMF in another channel. Stability of the obtained loops in every plot is then studied. Stability is considered as maintaining almost the same rotational pattern (profile) for the loops as well as the same overall trend.

Calculations of pulsation values as well as plotting of loops have been realized by MATLAB.

Frequency 3D mapping: EEG Spectrum amplitudes of every channel, related to the frequency bands: Delta (0.5-3.5), Theta (3.5-7.5), Alpha (7.5-12.5) and Beta (12.5-30), were calculated by Fourier Transform and mapped all over the channels of the scalp. Levels of spectrum amplitudes were indicated by colors: red, yellow, green and blue from highest to lowest, respectively. Patterns of 3D distribution were then studied.

III. Results and Discussion

Fig. 1 illustrates the intrinsic modes inherent in channel 1 of an autistic child EEG. The obtained components have different frequency contents. The component with the highest frequency is located in top of the figure while the component with the lowest frequency is located in bottom; the components are therefore ordered in a descending manner. These components hold essential information for distinguishing EEG autistic activity because they are the main constituents of measured EEG.

The obtained amplitude-modulated frequency-modulated IMFs have been extracted in a non-linear manner by EMD; this ensures the adaptive and data-driven properties of the procedure in the present study.

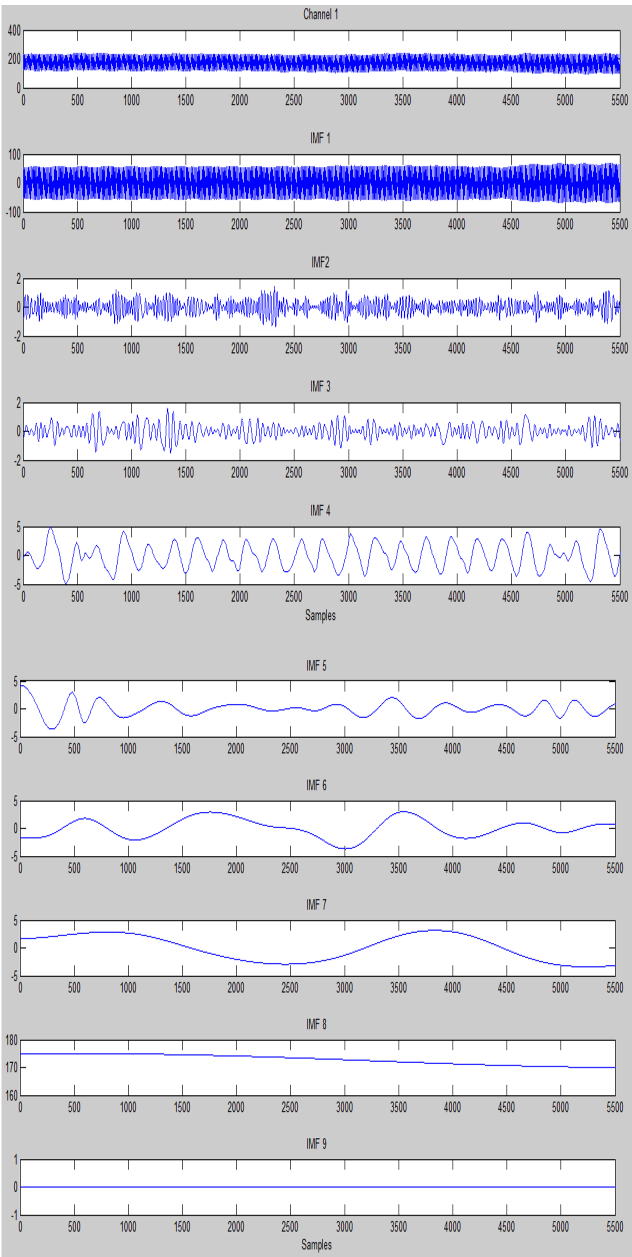

Fig. 1. The intrinsic modes inherent in channel 1 of an autistic child EEG.

Fig. 2 illustrates the IMF1 of channel 1 of a normal child with its corresponding normalized point-by-point pulsation function. It is essential to note that the followed procedure ensures pulsation independent calculation without being influenced by amplitude modulation.

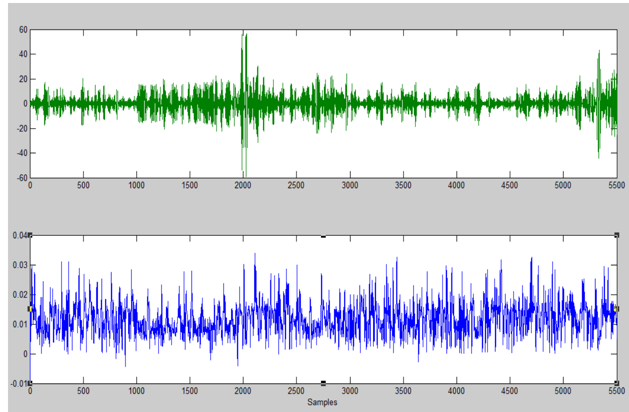

Fig. 2. The IMF1 of channel 1 of a normal child (top) with its corresponding point-by-point pulsation function (bottom).

Fig. 3a and Fig. 3b illustrate the plot of the local pulsation values of the first IMF of channel 3 versus those of the first IMF in channel 2 for a neuro-typical and an autistic child, respectively. The stability of the pulsation pattern in autistic child is obvious while it is absent in neuro-typical. In autism, the loop maintains almost the same rotational profile in a determined region. However, in normal case, the loop goes into random stochastic pathways. In autism case, this indicates an unusual functional neural connectivity between the two brain sites represented by channels 2 and 3. Basically, in normal cases, these two sites should not have the same pace or, in other terms, should not have highly synchronous activities.

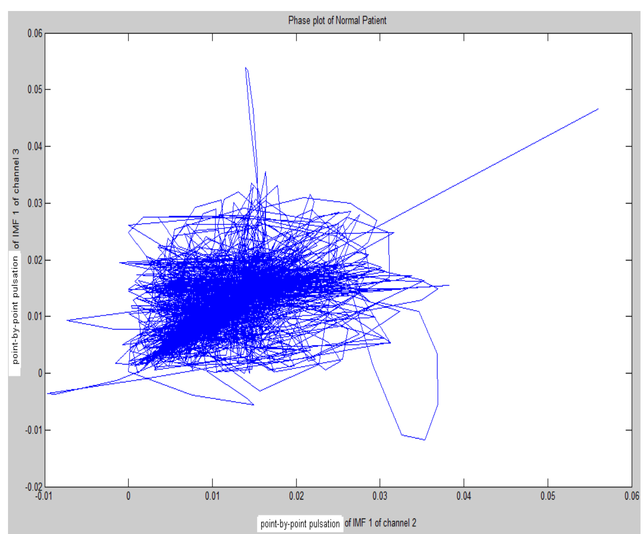

Fig. 3a. The plot of the local pulsation values of the first IMF of channel 3 versus the local pulsation values of the first IMF of channel 2 for a neuro-typical child.

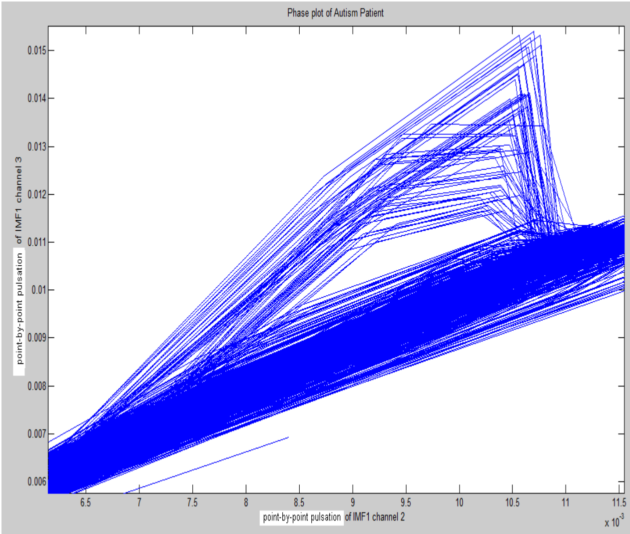

Fig. 3b. The plot of the local pulsation values of the first IMF of channel 3 versus the local pulsation values of the first IMF of channel 2 for an autistic child.

Fig. 4a and Fig. 4b illustrate the plot of the local pulsation values of the first IMF of channel 2 versus the local pulsation values of the first IMF of channel 1 for a neuro-typical and autistic child, respectively. The abnormal stability and functional neural connectivity are also evident in the illustrated loops. The stochastic pathways are more visible in the normal case than in the autistic condition. In autistic case, the loop is more determined with a more precise trend. In general, the result presented herein can indicate that a certain neural action is processed differently between an autistic and a normal child. The brain zones represented by channels 1 and 2 are rather working independently in normal child while they work mutually and synchronously in autistic child.

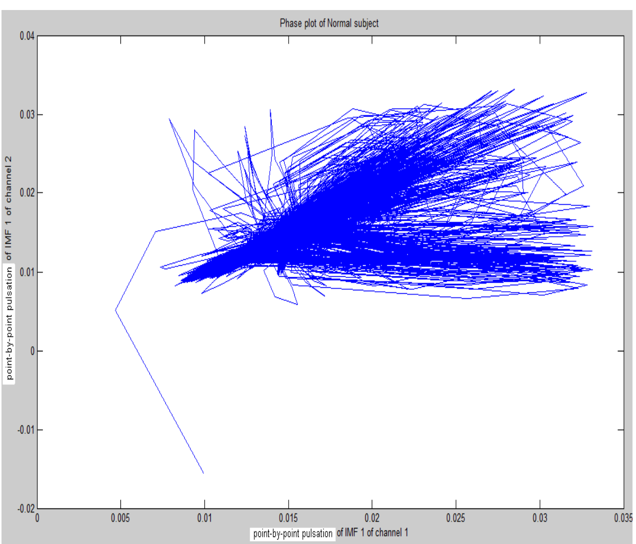

Fig. 4a. The plot of the local pulsation values of the first IMF of channel 2 versus the local pulsation values of the first IMF of channel 1 for a neuro-typical child.

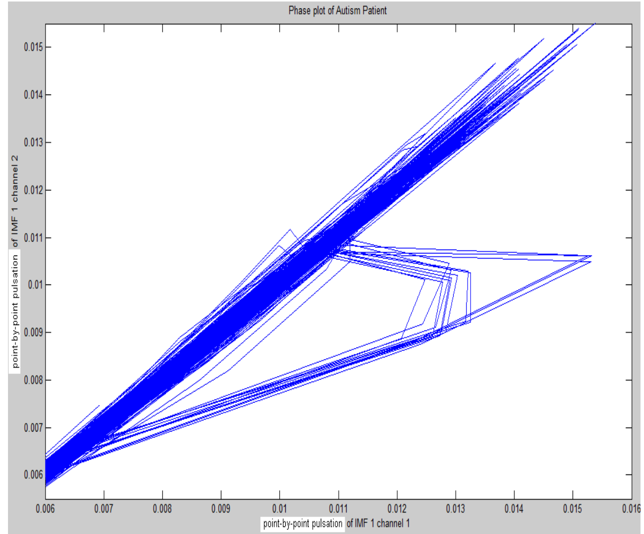

Fig. 4b. The plot of the local pulsation values of the first IMF of channel 2 versus the local pulsation values of the first IMF of channel 1 for an autistic child.

Fig. 5a and Fig. 5b illustrate the plot of the local pulsation values of the first IMF of channel 36 versus the local pulsation values of the first IMF of channel 37 for a neuro-typical and autistic child, respectively. The abnormal stability and functional neural connectivity are also evident in the illustrated loops.

Here again, it can be deduced that the brain zones represented by channels 36 and 37 are rather working independently in normal child while they work mutually and synchronously in autistic child; which can lead to a confusion in the processing of a certain neural action.

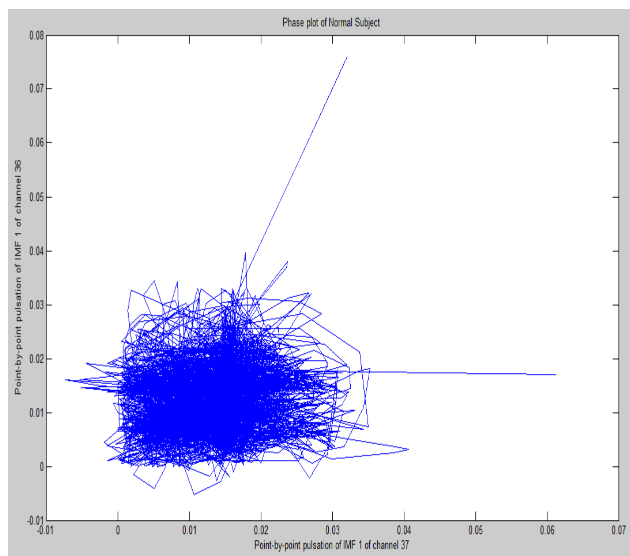

Fig. 5a. The plot of the local pulsation values of the first IMF of channel 36 versus the local pulsation values of the first IMF of channel 37 for a neuro-typical child.

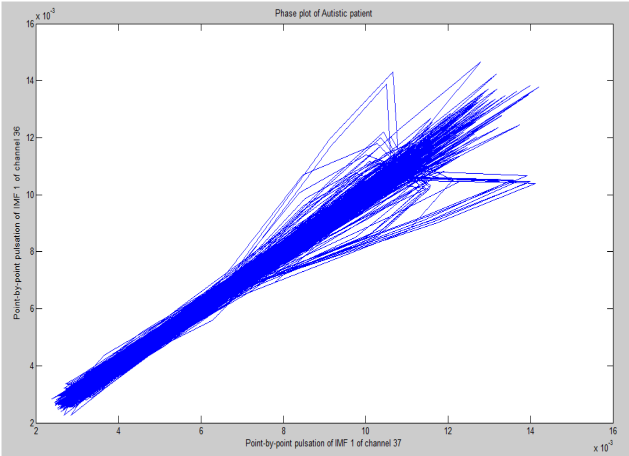

Fig. 5b. The plot of the local pulsation values of the first IMF of channel 36 versus the local pulsation values of the first IMF of channel 37 for autistic child.

The previous figures indicate an abnormal synchronization between brain sites at an autistic child. This pattern was found in all autistic volunteers studied in the present work compared to the neuro-typical ones. IMF1 is found to be mostly influenced; which means that the high frequency content in brain processes is rather affected by the odd connectivity. The other IMFs were partially influenced. However, the big difference was clearer in IMF1. Our findings are consistent with the physiological findings in the literature [3-5].

The differences, between normal and autistic states, in the level of coupling of the EEG activity of channels also imply differences in the frequency content of each channel signal. This is because, basically in normal cases, brain sites with different point-by-point pulsation values (local frequency values) will not have high inter-channel stability measure, and vice versa. This deduction is proved by Figures 6, 7, 8 and 9 where the distribution of frequency content is different between normal and abnormal cases. In neuro-typical cases, (Figure. 6 and 8), the frequency content varies more strongly than in autistic cases where large zones have the same color i.e. the same spectrum amplitude for the frequency bands Delta, Theta, Alpha and Beta (from left to right) (Figure. 7 and 9).

The more homogeneous distribution in autism might characterize an anomalous synchronous triggering in activities of several brain sites. This leads to a weak integration of information and huge distraction; which are the main features of autism disorder according to international behavioral evaluations.

The results show that the stability loops and the 3D mapping of frequency can be useful promising cursors that have the potential of indicating atypical characteristics in Autism spectrum. The main characteristics approached by the present study are the abnormal connectivity between a number of brain sites as well as the brain activity irregular distribution.

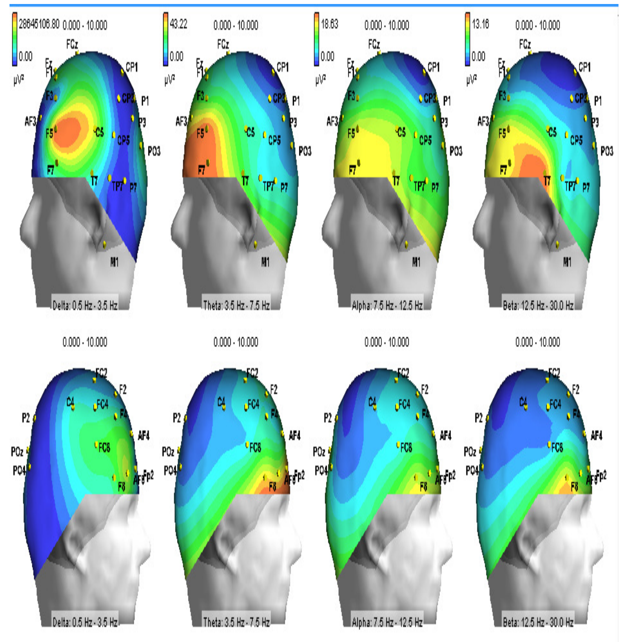

Fig. 6. The right and left views of 3D mapping of frequency bands Delta, Theta, Alpha and Beta (from left to right) for a neuro-typical child. Red, yellow, green and blue indicate spectrum amplitudes in a descending manner from highest to lowest values.

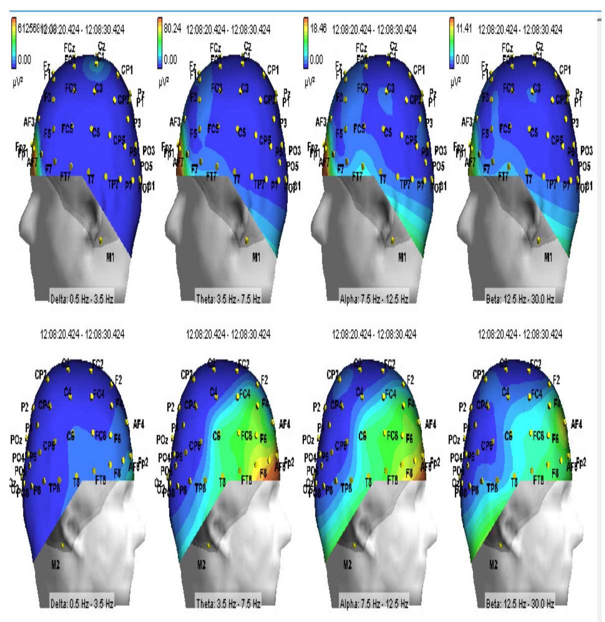

Fig. 7. The right and left views of 3D mapping of frequency bands Delta, Theta, Alpha and Beta (from left to right) for an autistic child. Red, yellow, green and blue indicate spectrum amplitudes in a descending manner from highest to lowest values.

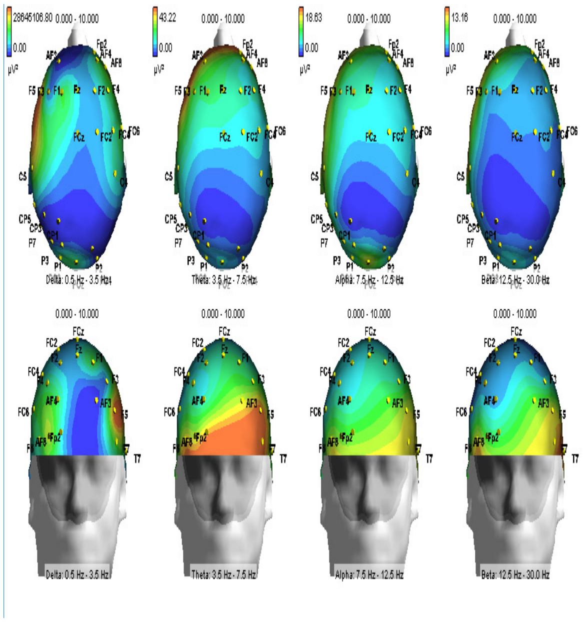

Fig. 8. The top and front views of 3D mapping of frequency bands Delta, Theta, Alpha and Beta (from left to right) for a neuro-typical child. Red, yellow, green and blue indicate spectrum amplitudes in a descending manner from highest to lowest values.

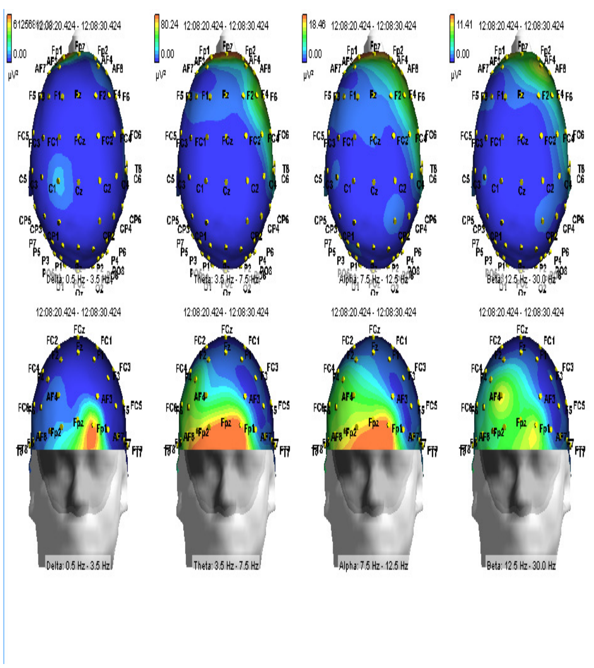

Fig. 9. The top and front views of 3D mapping of frequency bands Delta, Theta, Alpha and Beta (from left to right) for an autistic child. Red, yellow, green and blue indicate spectrum amplitudes in a descending manner from highest to lowest values.

IV. CONCLUSION

The inter-channel stability of pulsation plot and the distribution of frequency content all over the scalp are promising indicators to autism. They detect abnormal EEG activities and neural connectivity.

Future work will focus more on quantifying the characteristics of the plots in order to establish more robust criteria for quantitative diagnosis.

Acknowledgment

This study was conducted under the umbrella of a Scientific Research Support Fund (SRSF)-funded project/Ministry of Higher Education and Scientific Research, Jordan.

References

[1] Amira T M, Najati AS, Ramzi N: Diagnostic delay of autism in Jordan: review of 84 cases. Libyan J Med 2013, 8:21725.

[2] Ali S, Hamid B, Mohammad RM, Maryam N, Mohammad M:Detection of Abnormalities for Diagnosing of children with Autism Disorders Using of Quantitative Electroencephalography Analysis, J Med Syst 2012, 36:957-963.

[3] Barttfeld P, Wicker B, Cukler S, Navarta S, Lew S, Sigman M: A big-world network in ASD: dynamical connectivity analysis reflects a deficit in long-range connectios and an excess of short-range connections. Neuropsycologia 2011, 49:254-263.

[4] Duffy FH, Als H: A stable pattern of EEG spectral coherence distinguishes children with autism from neuro-typical controls- a large case control study. BMC Med 2012, 10:64.

[5] Burnette CP, Henderson HA, Inge AP, Zahka NE, S chwartz CB, Mundy PC: Anterior EEG asymmetry and the modifier model of autism. J Autism Dev Disord 2011, 41:1113-1124.

[6] Jun W, Jamie B, Lauren EE, Matthew WM, Yukari T, John AS: Resting state EEG abnormalities in autism spectrum disorders 2013, 5:24

[7] Ana C, Alexandre A, Owen C, Adam P W, Simon B-C and Howard R: Task-related functional connectivity in autism spectrum conditions: an EEG study using wavelet transform coherence. J Molecular Autism 2013, 4:1.

[8] Rami J O and Enas W A : Seizure classification in EEG signals utilizing Hilbert-Huang transform. BioMedical Engineering OnLine 2011, 10:38.

[9] Huang NE, Shen Z, Long SR, Wu MC, Shin HH, Zheng Q, Yen N-C, Tung CC, Liu HH: The empirical mode decomposition and Hilbert spectrum for nonlinear and non-stationary time series analysis. Proceedings - Royal Society. Mathematical, physical and engineering sciences; 1998. 454. 903:995.

[10] Enas Abdulhay, Abdelhay A, Kilani A, Shwyat L and Rousan S. , Development of Arduino based low cost neuro-feedback for ADHD, Biomed Research, 27, Computational Life Sciences and Smarter Technological Advancement,2016, 31-37.

[11] Ahmadlou M, Adeli H and Adeli A : Fractality and a wavelet-chaos-neural network methodology for EEG-based diagnosis of autistic spectrum disorder. J Clin Neurophysiol. 2010. 27(5):328-33.

[12] Abdulhay. E, et Baconnier. P, Stroke Volume Estimation is Better when Glotis is closed, /L'Estimation du Volume d'Ejection Par La Thoracocardiographie est Meilleure Quand la Glotte est Fermée/, Innovation and Research in Biomedical Engineering IRBM, 2008, 29 (5), 297-301.